Dynamics of wave point absorbers connected to a central floating platform

Thiago S. Hallak, José F. Gaspar, and C. Guedes Soares

Abstract—**In this paper, the nonlinear geometric constraints that arise naturally in hinged structures are investigated for floating multi-body wave point absorbers. A new method of constraint linearization is proposed and applied to a realistic case study. The method is based on generalized coordinates, and generates a robust first-order dynamic matrix to characterize the multi-degrees of freedom hydrodynamic system. The simulation outputs the motion response for all floating bodies, as well as the constraint force responses, among other parameters. The method requires knowledge of the geometries of the system but rather few assumptions, namely, to perform the linearization of constraints. The method is illustrated with the mechanical connection between three wave point absorbers to a central Floating Offshore Wind Turbine and on-board hydraulic Power-Take Off systems.**

Keywords—**Multi-use platforms, renewable energies offshore, nonlinear dynamics, nonlinear mechanics, response amplitude operators.**

I. INTRODUCTION

THE mathematical and numerical modelling of Wave Energy Converters (WECs) and WEC arrays is an essential step in the development of the wave energy industry. Various levels of physical complexity are reflected in the modelling of such dynamic systems, e.g. from the wave excitation pressure field on the WEC to the mooring system dynamics, from the wave radiation properties of the WEC to the Power Take-Off (PTO) dynamics, due to viscous effects, and so on. Oftentimes, the term *nonlinear* or *nonlinearity* is employed, because the mathematical modelling of the system brings dynamic equations to be solved that are indeed nonlinear.

In the case of wave point absorbers interconnected, or connected to a central floating platform, the connection is normally performed employing hinged-arms. Because multi-body hydrodynamics is usually accounted for from a global perspective, the appearance of nonlinear geometric constraints is unavoidable (a fact that will be better explained in the next section). It is a challenge to model, both mathematically and numerically, the exact multi-degrees of freedom coupled dynamics of constrained floating multi-body systems.

The theoretical analysis of floating systems with multiple underwater geometries started over 50 years ago, but the application was rather limited to rigid-body structures with multiple underwater geometries, as it is the case of catamarans and floating stations [1]. Nevertheless, important conclusions were drawn in regards to the interactions between the different hulls, for instance, that those interactions may be particularly strong, indeed nearly singular depending upon wavelength and the spacing between hulls.

The analysis of multi-body floating systems for application in wave energy farms started by demonstrating the generalization of hydrodynamic wave-structure interaction formulation for multi-body systems [2,3]. The development of the field brought many important contributions to multi-body hydrodynamics, e.g. [4–6], whereas many conclusions have been reviewed and summarized in [7]. Those studies provide deep insight into the interactions within WEC arrays composed of identical floating bodies. Today, the state-of-the-art of WECs and WEC arrays hydrodynamic modelling also encompass optimisation and control techniques, for instance, as done by [8,9].

Recently, researchers have been looking into coupling WECs with Floating Offshore Wind Turbines (FOWTs), mainly due to the accelerated development of the offshore wind industry [10]. However, hybrid wind-wave

The first author has a PhD Scholarship by the Portuguese Foundation for Science and Technology (Fundação para a Ciência e Tecnologia – FCT), under contract No. SFRH/BD/145602/2019. This work contributes to the Strategic Research Plan of the Centre for Marine Technology and Ocean Engineering (CENTEC), which is financed by the Portuguese Foundation for Science and Technology (Fundação para a Ciência e Tecnologia - FCT) under contract UIDB/UIDP/00134/2020, and the project "Variable geometry Wave Energy Conversion system for floating platforms" funded by FCT under contract PTDC/EME-REN/0242/2020.

T. S. Hallak, J. F. Gaspar, and C. Guedes Soares are with the Centre for Marine Technology and Ocean Engineering (CENTEC), Instituto Superior Técnico, Universidade de Lisboa, 1049-001, Lisboa, Portugal (e-mail: thiago.hallak@centec.tecnico.ulisboa.pt, jose.gaspar@centec.tecnico.ulisboa.pt, c.guedes.soares@centec.tecnico.ulisboa.pt).

Digital Object Identifier: https://doi.org/10.36688/ewtec-2023-496

technology using wave point absorbers is still in TRL 4, meaning that hybrid wind-wave technology has been validated in laboratories [11-14]. A collection of analyses may be found in recent bibliography considering different concepts.

The works done by [15-18], for instance, consider the DeepCWind FOWT [19,20] as a central platform, which is a validated model of the semi-submersible type. This type of configuration has the main advantages of i) being more versatile in regards to the water depth, and ii) it allows both a greater deck load and larger deck area in comparison to the other floating types. The latter advantage is, indeed, key for the coupling of WECs and hydraulic PTOs on-board. Nevertheless, it is worth mentioning that other configurations had also been considered in numerical analysis for hybrid wind-wave systems, e.g. the NREL OC5 spar platform [21], the braceless semi-submersible FOWT [22], and the MIT-NREL TLP [23].

In this paper, a new method based on generalized coordinates is shown to generate a robust dynamic matrix for the simulation of mechanically-constrained floating multi-body systems. The method is here demonstrated in the frequency domain, but it is easily extendable to the time domain. The method requires knowledge on the exact geometries of the system, but rather few assumptions. Insights are given into how to model the mechanical constraints of complex multi-body systems. The method is illustrated with the following case study: The connection between three WECs to a central floating platform and hydraulic PTOs. The central platform is an adapted version of the DeepCWind semi-submersible with a higher draft and displacement for a more powerful, 10 MW wind turbine.

II. MATHEMATICAL MODELLING

In this section, the basis of the mathematical model developed to analyse mechanically-constrained floating multi-body systems is presented in detail. The mathematical model has been developed for the application in various classes of floating multi-body systems, especially WEC arrays, hybrid wind-wave technology and other Multi-Use Platform (MUP) types.

Within the method's framework, different geometries may be considered, as well as different mechanical constraints, different amounts of floating bodies, different exciting forces, and so on. The major difficulty is normally analytical, namely, in the evaluation of the linear combinations that relate global motions and global forces with generalized motions and generalized forces. Because there are many parameters and linearizations to be performed, the formulae in sub-section II.C – Hydraulic PTOs – is given for the case study at hand, only, whereas the other sub-sections contain rather generic formulae. In the formulae that will follow, square brackets stand for matrixes, curly brackets stand for arrays, and bold stands for vectors.

A. Multi-Body Hydrodynamics

The hydrodynamic problem of wave-structure interaction between planar Airy waves and a rigid-body structure is usually represented, physically, by a mass-spring-damper system or, mathematically, by a 2nd-order linear Ordinary Differential Equation (ODE). If all modes of motion are considered, the dimension of the ODE system is 6. In a global perspective, when considering different floating structures, a first generalization is obtained by increasing the dimension of the linear system and the number of degrees of freedom (dof) accordingly. Then, the addition of constraints reduces the number of degrees of freedom in the system.

On the one hand, at present, commercial and open-source hydrodynamic software are able to evaluate the hydrodynamic forces related to the diffraction and radiation wave effects around multiple floating bodies. Though the possible amount of different underwater geometries is normally a limitation of the software, the hydrodynamic coefficients are given in terms of added mass, damping and excitation force coefficients rather straightforwardly for a global reference. On the other hand, the solution of the multi-body dynamic interaction is not straightforward if nonlinear mechanical constraints are present.

The assumption of linear separation of potentials is also considered in multi-body solvers to obtain the radiation and diffraction potentials separately. Because potential flow is assumed, the velocity of a fluid particle is given by the gradient of the real part of total potential Φ, which is the sum of diffraction and radiation wave potentials. Those may be written in the complex form

$$\Phi \equiv \Phi(\boldsymbol{F}) = |\Phi(\boldsymbol{F})| \exp i\omega t = \Phi_{\mathrm{D}} + \Phi_{\mathrm{R}} \,, \tag{1}$$

where $\boldsymbol{F} = (x_F, y_F, z_F)$= the position vector of fluid particle, Φ_{D} = the diffraction potential, and Φ_{R} = the radiation potential.

Assuming the mechanical constraints of the system to be holonomic, as it is the case of hinged structures, then the dynamic equations of the system can be written with application of Newton-Euler method. In the frequency domain, by assuming potential flow and linear Airy waves incidence, the multi-body wave-structure interaction can be written as

$$\begin{gathered}[M + M_{\mathrm{rad}}(\omega)]\{\ddot{x}\} + [B_{\mathrm{add}} + B_{\mathrm{rad}}(\omega)]\{\dot{x}\} + \\ \left[C_{\mathrm{hyds}}\right]\{x\} = \{f_{\mathrm{e}}(\omega)\} + \{f_{\mathrm{c}}\} \,,\end{gathered} \tag{2}$$

where M = mass-inertia matrix; $M_{\mathrm{rad}}(\omega)$ = added mass matrix obtained from the radiation potential; $B_{\mathrm{rad}}(\omega)$ = radiation damping matrix; B_{add}= added damping matrix; C_{hyds}= hydrostatic restoring matrix; x= global coordinates; $f_{\mathrm{e}}(\omega)$= wave excitation force array; and f_{c}= constraint force array.

The relations between the potentials in Eq. (1) and the coefficients in Eq. (2) may be found in [7]. Clearly, the major difference between Eq. (2) and the dynamic equation of a floating rigid-body is the unknown array of constraint forces. In a Newtonian perspective, the constraint forces appear as global forces in the interconnection endpoints of the different rigid bodies, and the position of those points vary over time. For a hinged-arm, the geometric constraint equation, though holonomic, is nonlinear, because it is a second-degree polynomial in terms of the global motion variables and in the global reference frame O_{xyz}, meaning that the distance between endpoints is constant, and equals the length of the arm

$$L_{PQ} \equiv \|\boldsymbol{P},\boldsymbol{Q}\| \Rightarrow \\ \left(L_{PQ}\right)^2 = \left(x_P - x_Q\right)^2 + \left(y_P - y_Q\right)^2 + \left(z_P - z_Q\right)^2, \quad (3)$$

where $\boldsymbol{P} = (x_P, y_P, z_P)$ and $\boldsymbol{Q} = \left(x_Q, y_Q, z_Q\right)$= the position vectors of the interconnection endpoints (hinged or fixed connection), and L_{PQ}= the length of the arm. To solve the nonlinear system of Equations (2) and (3) is a hard task to perform both analytically and numerically.

B. Constraint Linearization

The same hydrodynamic problem stated above is here solved in a different way, namely, by performing a constraint linearization that gives away nonlinear Eq. (3). For that, all mechanical constraints are accounted, though in a linear fashion. The idea is to obtain, for a system with N interconnected bodies, a linear set of $6N$ equations and variables. First, a robust linearization of the motion variables is performed: the $6N$ motion variables are written in terms of $6N - K$ generalized coordinates, where K is the number of constraints, or

$$\begin{cases} x_1 = G_1(w_1,w_2,\dots,w_{6N-K}) = \sum_{j=1}^{6N-K} g_{1j} w_j \\ x_2 = G_2(w_1,w_2,\dots,w_{6N-K}) = \sum_{j=1}^{6N-K} g_{2j} w_j \\ \dots \\ x_{6N} = G_{6N}(w_1,w_2,\dots,w_{6N-K}) = \sum_{j=1}^{6N-K} g_{(6N)j} w_j \end{cases}, \quad (4)$$

where w_j= the j-th generalized coordinate; and g_{ij}= the coefficient of the linear combination G_i representing the influence of generalized coordinate j on the global motion of mode i.

The remaining simplifications regard the constraint forces. The linearization is performed considering that the direction of the constraint forces remains the same at all times, corresponding as well to the equilibrium position of the system. Then, a total of K generalized constraint forces shall appear, which may depend on the generalized motion variables as well, and also its first and second-order derivatives, as it is the case of hydraulic PTOs, or

$$\{f_c\} = \\ \{f_c(w_1, \dot{w}_1, \ddot{w}_1 \dots, w_{6N-K}, \dot{w}_{6N-K}, \ddot{w}_{6N-K}, y_1, \dots, y_K)\}, \quad (5)$$

and

$$\begin{cases} f_{c1} = H_1(w_1,\dot{w}_1,\ddot{w}_1\dots,w_{6N-K},\dot{w}_{6N-K},\ddot{w}_{6N-K},y_1,\dots,y_K) \\ f_{c2} = H_2(w_1,\dot{w}_1,\ddot{w}_1\dots,w_{6N-K},\dot{w}_{6N-K},\ddot{w}_{6N-K},y_1,\dots,y_K) \\ \dots \\ f_{c(6N)} = H_{6N}(w_1,\dot{w}_1,\ddot{w}_1\dots,w_{6N-K},\dot{w}_{6N-K},\ddot{w}_{6N-K},y_1,\dots,y_K) \end{cases}. \quad (6)$$

Thus,

$$f_{ci} = \sum_{j=1}^{6N-K}\left(h_{ij}^{(0)} w_j + h_{ij}^{(1)} \dot{w}_j + h_{ij}^{(2)} \ddot{w}_j\right) + \\ \sum_{j=1}^{K} h_{i(6N-K+j)} y_j, \; i = 1, \dots, 6N, \quad (7)$$

where f_{ci}= the constraint force acting on global motion variable i; y_j= the j-th generalized force; $h_{i(6N+j)}$= the coefficient of linear combination H_i representing the influence of the j-th generalized force on the global constraint force at mode i, and $h_{ij}^{(k)}$= the coefficient of the linear combination H_i representing the influence of the k-th derivative of the generalized motion variable j on the global constraint force at mode i.

The substitution of Equations (4) and (7) back into Eq. (1) leads to a $6N \times 6N$ linear system of the form

$$[A]\{(\ddot{w},y)\} + [B]\{(\dot{w},y)\} + [C]\{(w,y)\} = \{f_e(\omega)\}, \quad (8)$$

where $A \equiv A(\omega)$ and $B \equiv B(\omega)$.

Equation (8) is equivalent in form to the dynamic equation of a floating rigid-body, however, with a higher dimension and different block structure. Equation (8) may be solved in the frequency domain rather straightforwardly. It may also be adapted and solved in the time domain considering the Cummins Equation [24,25], whereas the time domain solution may include several additional forces in the right-hand side (RHS), e.g. mooring forces (essential to provide station-keeping in time domain models), aerodynamic forces, among others.

C. Hydraulic PTOs

This sub-section shows how to evaluate the matrixes in Eq. (8) for the case where wave point absorbers are connected to a single central platform by means of hinged-arms and hydraulic PTOs.

Assuming that the connections between arms and WECs are totally rigid, and that the relative motion between the arms and the central platform are functions of piston motion inside the hydraulic PTO, then it is possible to write all motion variables as function of the 6 modes of motion of the central platform, plus the $N_{\mathrm{WEC}} = N - 1$ dof corresponding to the motions of the hydraulic pistons, where N_{WEC}= the amount of WECs connected to the central platform. In the present case, the number of dofs is, therefore, $6 + N_{\mathrm{WEC}}$, and the number of constraints is determined by $6N - 6 - N_{\mathrm{WEC}} = 5N_{\mathrm{WEC}}$. Thus, there must be 5 constraint force variables per WEC.

The evaluation of the linear functions G depend on the geometries of the system and the set of generalized coordinates

$$\{w\} = \{w_1, w_2, \dots, w_{6+N_{\mathrm{WEC}}}\}. \quad (9)$$

Then,

$$\begin{matrix} x_1 = w_1 \Rightarrow g_{11} = 1, g_{1j} = 0, j \neq 1 \\ \dots \\ x_6 = w_6 \Rightarrow g_{66} = 1, g_{6j} = 0, j \neq 6 \\ x_7 = G_7(w_1, \dots, w_6, w_{PTO1}) = \sum_{j=1}^{6N-K} g_{7j} w_j \\ \dots \\ x_{6N} = G_{6N}(w_1, \dots, w_6, w_{PTON_{\mathrm{WEC}}}) = \sum_{j=1}^{6N-K} g_{(6N)j} w_j \end{matrix}. \quad (10)$$

While G_j depends only on the geometries of the system, H_j depends on the model of forces and moments considered (e.g. the axial direction of the hinges) and the fact that the hinged-arm may share many contact points with the central platform, not just one. Therefore, the dynamic balance of the arm is required to properly evaluate the combinations H_j. The PTO model is also required, because the hydraulic forces act on the generalized modes. For instance, if the PTO is aligned with the vertical line, the vertical contact force acting on the platform around the PTO is given by the reaction of the force acting on the piston, that is

$$f_{PTOz} = \mu \ddot{w}_{PTO} + \beta \dot{w}_{PTO} + \kappa w_{PTO}, \quad (11)$$

where μ= the supplementary mass, or inertial parameter of the PTO; β= the damping of the PTO; and κ= the stiffness coefficient of the PTO.

Then, the contact forces acting on the platform around the hinge point $\boldsymbol{P}$ are evaluated based on $f_{\mathrm{PTO}z}$ and the remaining 5 constraining forces acting on the hinged-arm that satisfy the dynamic balance of the arm: $\{f_{PTOx}, f_{PTOy}, f_{Qx}, f_{Qy}, f_{Qz}\}$ is the set of 5 generalized forces, per WEC that were needed. Then,

$$\{f_{\mathrm{c}}\} = \left\{ f_{\mathrm{c}} \begin{pmatrix} w_{PTO\,j}, \dot{w_{PTO}}_j, \ddot{w_{PTO}}_j, \\ f_{PTOx\,j}, f_{PTOy\,j}, f_{Qx\,j}, f_{Qy\,j}, f_{Qz\,j} \end{pmatrix} \right\}. \quad (12)$$

If the weight of the arm is neglected, the dynamic balance of the arms is given by

$$\boldsymbol{f_{PTO}} + \boldsymbol{f_P} + \boldsymbol{f_Q} = \boldsymbol{0}, \quad (13)$$

where $\boldsymbol{f_{PTO}} = (f_{PTOx}, f_{PTOy}, f_{PTOz})$, $\boldsymbol{f_P} = (f_{Px}, f_{Py}, f_{Pz})$ and $\boldsymbol{f_Q} = (f_{Qx}, f_{Qy}, f_{Qz})$.

Equations (12) and (13) are linear in terms of motion and force variables, and allow to write the global forces in $\{f_c\}$, but not the global moments, whereas these depend, further, on the hinge models, for many types of hinges may be considered.

D. Transfer Functions

In this sub-section, Eq. (8) is solved for the case where the wave excitation force corresponds to a harmonic excitation of a given frequency ω. In the frequency domain, it is straightforward to evaluate the complex transfer functions, or Response Amplitude Operators (RAOs) and Response Phase Operators (RPOs), or complex RAOs. The first-order excitation of a given incoming Airy wave is given by

$$f_{ei}(\omega) = F_i(\omega)\cos(\omega t + \varphi_i), \; i = 1, \dots, 6N, \quad (14)$$

where F_i= the amplitude of the wave excitation force at global mode i; and φ_i= its phase relative to Φ.

Equation (14) is equivalent to

$$f_{ei}(\omega) = \mathrm{Re}\{F_i(\omega)\exp i(\omega t + \varphi_i)\}, \; i = 1, \dots, 6N, \quad (15)$$

Then, a harmonic solution is to be found by substituting

$$(w, y) = \begin{cases} W_j \cos(\omega t + \psi_j), & j = 1, \dots, 6N - K \\ Y_j \cos(\omega t + \psi_j), & j = 6N - k + 1, \dots, 6N \end{cases} \quad (16)$$

in Eq. (8), or

$$(w, y)_j = \begin{cases} \mathrm{Re}\{W_j \exp i(\omega t + \psi_j)\}, & j = 1, \dots, 6N - K \\ \mathrm{Re}\{Y_j \exp i(\omega t + \psi_j)\}, & j = 6N - k + 1, \dots, 6N \end{cases}, \quad (17)$$

then,

$$(\dot{w, y})_j = \begin{cases} \mathrm{Re}\{i\omega W_j \exp i(\omega t + \psi_j)\}, & j = 1, \dots, 6N - K \\ \mathrm{Re}\{i\omega Y_j \exp i(\omega t + \psi_j)\}, & j = 6N - k + 1, \dots, 6N \end{cases}, \quad (18)$$

and

$$(\ddot{w, y})_j = \begin{cases} \mathrm{Re}\{-\omega^2 W_j \exp i(\omega t + \psi_j)\}, & j = 1, \dots, 6N - K \\ \mathrm{Re}\{-\omega^2 Y_j \exp i(\omega t + \psi_j)\}, & j = 6N - k + 1, \dots, 6N \end{cases}, \quad (19)$$

where W_j = the response amplitude of motion in generalized mode j; Y_j= the response amplitude of the generalized force j; and ψ_j= their phase.

Substituting Equations (15) to (19) back into Eq. (8), a new form is attained:

$$\begin{aligned} \mathrm{Re}\left\{\left[-\omega^2[A] + i\omega[B] + [C]\right] \cdot \{(W, Y)\exp i(\omega t + \psi)\}\right\} \\ = \mathrm{Re}\{F(\omega)\exp i(\omega t + \varphi)\}. \end{aligned} \quad (20)$$

Because oscillatory motion is concerned, it is possible to look at the mathematical problem in the following way: The left-hand side (LHS) and RHS of Eq. (8) assume real values only, but they may be seen as the real parts of the complex numbers inside brackets shown in Eq. (20). Even though there are infinite complex numbers with the same real part, when writing the complex numbers as in Euler's formula, it is clear they oscillate with the same frequency ω. If the complex numbers are not the same but have the same real part at one instant, then there is another instant where they do not share the same real part. Thus, the only possible solution is that the complex numbers in the LHS and RHS must be the same, that is,

$$\left[-\omega^2[A]+i\omega[B]+[C]\right]\cdot\{(W,Y)\exp i(\omega t+\psi)\}=\{F(\omega)\exp i(\omega t+\varphi)\}\,. \tag{21}$$

Expanding the Euler's formulae, a solution is numerically obtained by solving the linear system

$$\begin{bmatrix} C-\omega^2 A & -\omega B \\ \omega B & C-\omega^2 A \end{bmatrix}\cdot\begin{Bmatrix}(W,Y)\cos\psi\\(W,Y)\sin\psi\end{Bmatrix}=\begin{Bmatrix}F(\omega)\cos\varphi\\F(\omega)\sin\varphi\end{Bmatrix}. \tag{22}$$

Mathematically, a solution to the system above is given by

$$\begin{Bmatrix}(W,Y)\cos\psi\\(W,Y)\sin\psi\end{Bmatrix}=\Lambda^{-1}\begin{Bmatrix}F(\omega)\cos\varphi\\F(\omega)\sin\varphi\end{Bmatrix}, \tag{23}$$

where

$$\Lambda=\begin{bmatrix} C-\omega^2 A(\omega) & -\omega B(\omega) \\ \omega B(\omega) & C-\omega^2 A(\omega) \end{bmatrix}, \tag{24}$$

given that the determinant of Λ is not zero. However, it is important to mention, linear solvers may be more accurate by solving Eq. (22) than the direct calculation by matrix inversion, especially for near-singular matrixes, that appear, for instance, when one or more modes of the system are not active (e.g. no forces nor motions in yaw).

Finally, the complex RAOs are given by

$$(W_j,Y_j)=\sqrt{\left((W_j,Y_j)\cos\psi_j\right)^2+\left((W_j,Y_j)\sin\psi_j\right)^2},\quad j=1,\dots,6N\,, \tag{25}$$

and

$$\psi_j=\operatorname{atan}\left(\frac{(W_j,Y_j)\sin\psi_j}{(W_j,Y_j)\cos\psi_j}\right),\ j=1,2,\dots,6N\,, \tag{26}$$

where the inverse tangent function considers the 4 quadrants of the Cartesian plane (or, the signs of both numerator and denominator in Eq. (26)).

Last but not least, the global motion responses are also obtained in the form of complex RAOs, by combining the complex solutions of Equations (25) and (26) according to Eq. (4).

III. ANALYSIS

The analysis is conducted for a hybrid wind-wave system consisting of a semi-submersible FOWT, namely the adapted version of the DeepCWind platform, coupled with 3 wave point absorbers, as shown in Fig. 1. The adaptation was made for the accommodation of a 10 MW wind turbine, that is, near the market standard of FOWT today. Figure 1 illustrates the size and shape of the WECs and the arms' length in comparison to the platform, but without reproducing them in scale.

The results in this section are shown for 10 meter diameter WECs of conical form and square tip angle. The

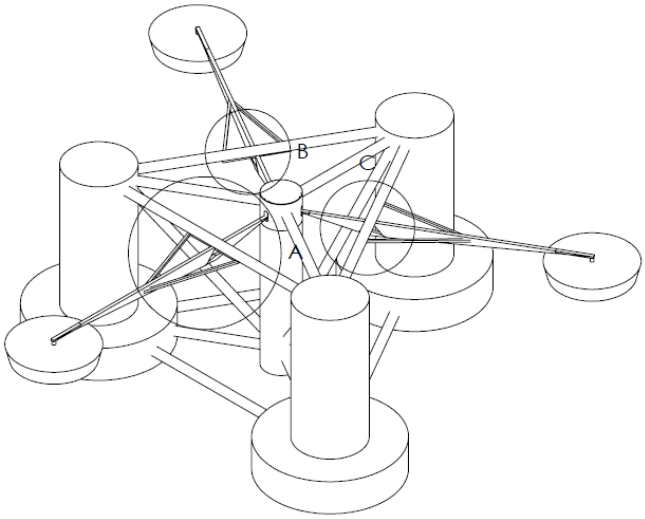

Fig. 1. Illustration of the hybrid wind-wave energy system consisted on the adapted version of the DeepCWind for a 10.0 MW wind turbine and 3 wave point absorbers. (Grant contract PTDC/EME-REN/0242/2020).

distance between the brace of the FOWT and the centre of the WEC, or the horizontal distance between points P and Q, is 20 meters. The results are plotted in Fig. 2 in the form of FOWT pitch RAOs, because pitch motion is essential to the proper functioning and higher efficiency of the turbine, it is a rather important aspect to look out for when studying hybrid wind-wave systems. For comparison, the pitch RAO of the system is plotted against the single-body RAO of the platform and the RAO when only hydrodynamic coupling is accounted for. The results are drawn for 30 frequencies equally distant. In further analysis, more frequencies should be employed so the plots do not suffer from the straight lines' discretization.

In Fig. 2, the pitch RAOs demonstrate that both hydrodynamic interaction and mechanical interaction do affect the dynamic behaviour of the central platform in the pitch motion.

Regarding the hydrodynamic interaction, because the WECs are much smaller than the central platform, the pitch of the platform starts to respond in smaller waves when compared to the single-body platform, i.e. at the high-frequency range. In the low-frequency range, energy is being captured by the resonant mode of the central platform due to wave interactions, evidenced by the amplification of response around the period of 30.0 seconds, whereas within the wave-frequency range, the hydrodynamic interaction leads to smaller pitch motions.

Figure 2 shows that, when also considering the mechanical constraints of the system, the energy around the resonance can be mitigated due to the coupled dynamics with the WEC-PTO system. The influence is clear from the low- to the wave-frequency range, whereas in the high-frequency range the influence is rather small, because at high frequencies inertia dominates but the inertia of the WECs and PTO is indeed much smaller than the inertia of the FOWT.

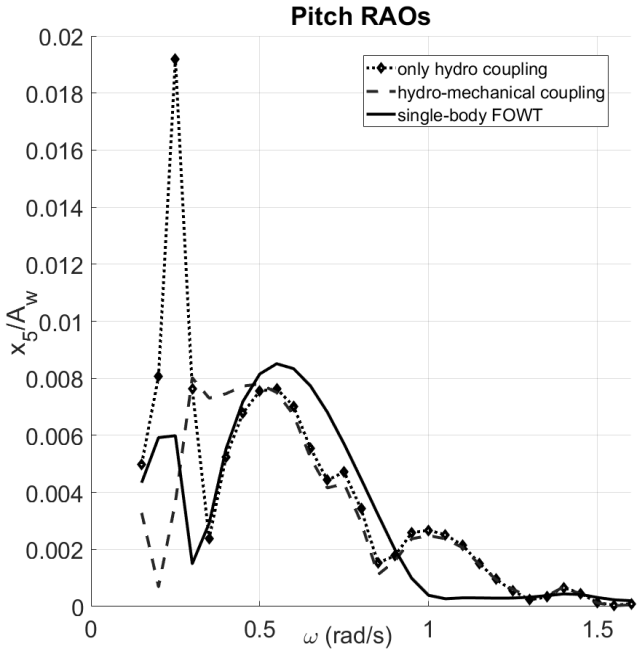

Fig. 2. FOWT Pitch RAOs in different scenarios. (Grant contract PTDC/EME-REN/0242/2020).

Last but not least, the results in Fig. 2 show, overall, that the averaged pitch motion of the FOWT may be mitigated depending on a suitable hybrid system.

IV. CONCLUSIONS

In this paper, a method based on generalized coordinates is presented in detail. The formulation is put in a rather generic way for the application in various types of WEC arrays, hybrid wind-wave systems and other MUPs. The application of the new formulation is illustrated with an example of practical interest, that is, of a 10 MW FOWT coupled with wave point absorbers.

The application of the method reduced the complexity of the hydrodynamic system by giving away the nonlinear geometric constraints equation that appears due the connection of the different floating bodies. The formulation accounts for the whole set of linear 1st order influences of all hydrodynamic and mechanical interactions involved, by considering the exact geometries and the hydraulic PTO parameters.

The section on analysis presented rather preliminary results for the investigated case study. The results, though, illustrated the time efficiency of the method. The numerical solutions are obtained by solving a linear system, which may be performed fast even in a home computer. Due to the time efficiency of the method, it can be used, for instance, in optimization algorithms for the best selection of PTO parameters and wave point absorbers geometries for different types of central platforms.

Lastly, to exemplify how the method can be used in optimization, it is straightforward to treat many parameters so far considered (contact points, inertia models, PTO models, etc.) as variables for optimization. Then, providing the constraints (e.g. maximum stroke, maximum loads, maximum PTO pressure, etc.) and objective, or multi-objective function (e.g. maximization of WECs' energy output/minimization of FOWT pitch motion), nonlinear optimization algorithms shall find the best values for the optimization variables. The drawback of this method is that, because the multi-body hydrodynamic coefficients are required, it is necessary perform a diffraction/radiation run for each underwater geometry analysed, which varies when a different WEC shape or diameter is selected, or due to different spacing between WECs and central platform. Still, given a good preliminary set of underwater geometries, it may be possible as well to perform a finite set of optimization runs allowing the user to select an optimum WEC-PTO model for its central platform.

REFERENCES

[1] M. Ohkusu, "On the heaving motion of two circular cylinders on the surface of a fluid," *Rep. Res. Inst. Appl. Mech.*, vol. 27(58), pp. 167–185, 1969.

[2] K. Budal, "Theory for absorption of wave power by a system of interacting bodies," *J. Ship Res.*, vol. 21(4), 248, 1977.

[3] J. Falnes, "Radiation impedance matrix and optimum power absorption for interacting oscillators in surface waves," *Appl. Ocean Res.*, vol. 2(2), pp. 75-80, 1980.

[4] P. McIver, "Some hydrodynamic aspects of arrays of wave-energy devices," *Appl. Ocean Res.*, vol. 16, pp. 61-69, 1994.

[5] S. A. Mavrakos, and P. McIver, "Comparison of methods for computing hydrodynamic characteristics of arrays of wave power devices," *Appl. Ocean Res.*, vol.19, pp. 283-291, 1997.

[6] S. Chakrabarti, "Hydrodynamic interaction forces on multi-moduled structures," *J. Ship Res.*, vol. 21(4), 1037-1063, 1999.

[7] J. N. Newman, "Wave effects on multiple bodies," *Hydrodyn. Ship Ocean Eng.*, vol. 3, pp. 3-26, 2001.

[8] C. J. Fitzgerald, "Optimal configurations of arrays of wave-power devices," Master thesis, National University of Ireland, Cork, Ireland, 2006.

[9] P. Balitsky, "Modelling controlled arrays of wave energy converters," Master thesis, National University of Maynooth, Ireland, 2013.

[10] H. M. Diaz, and C. Guedes Soares. Review of the current status, technology and future trends of offshore wind farms. *Ocean Eng.*, vol. 209, 107381, 2020

[11] T. S. Hallak, J. F. Gaspar, M. Kamarlouei, M. Calvário, M. J. G. C. Mendes, F. Thiebaut, and C. Guedes Soares, "Numerical and experimental analysis of a hybrid wind-wave floating platform's hull," in *Proc. ASME 37th Int. Conf. Ocean Offshore Arct. Eng.*, V11AT12A047, Madrid, Spain, Jun, 2018.

[12] J. F. Gaspar, T. S. Hallak, and C. Guedes Soares, "Semi-submersible platform concept for a concentric array of wave energy converters," In *Advances in Renewable Energies Offshore, C. Guedes Soares (Ed.),* Taylor & Francis Group, pp. 307-314, London, 2018.

[13] M. Kamarlouei, J. F. Gaspar, M. Calvário, T. S. Hallak, C. Guedes Soares, M. J. G. C. Mendes, and F. Thiebaut, "Prototyping and wave tank testing of a floating platform with point absorbers," in *Advances in Renewable Energies Offshore, C. Guedes Soares (Ed.),* Taylor & Francis Group, pp. 422-428, London, 2018.

[14] M. Kamarlouei, J. F. Gaspar, M. Calvário, T. S. Hallak, M. J. G. C. Mendes, and F. Thiebaut, "Experimental analysis of wave energy converters concentrically attached on a floating offshore platform," *Renew. Energ.*, vol. 152, pp. 1171-1185, 2020.

[15] T. S. Hallak, D. Karmakar, and C. Guedes Soares, "Hydrodynamic performance of semi-submersible FOWT

combined with point-absorber WECs," In *Developments in Maritime Technology and Engineering. CRC Press*, pp. 577-585, 2021.

[16] Y. Si, Z. Chen, W. Zeng, J. Sun, D. Zhang, X. Ma, and P. Qian, "The influence of power take-off control on the dynamic response and power output of combined semi-submersible floating wind turbine and point-absorber wave energy converters," *Ocean Eng.*, vol. 227, 108835, 2021.

[17] H. R. Ghafari, H. Ghassemi, and G. He, "Numerical study of the Wavestar wave energy converter with multi-point-absorber around DeepCWind semisubmersible floating platform," *Ocean Eng.*, vol. 232, 109177, 2021.

[18] Z. Chen, J. Yu, J. Sun, M. Tan, S. Yang, Y. Ying, P. Qian, D. Zhang, and Y. Si, "Load reduction of semi-submersible floating wind turbines by integrating heaving-type wave energy converters with bang-bang control," *Front. Energy Res.*, vol. 10, 929307, 2022.

[19] A. N. Robertson, F. Wendt, J. M. Jonkman, W. Popko, H. Dagher, S. Gueydon, J. Qvist, F. Vittori, J. Azcona, E. Uzunoglu, C. Guedes Soares, R. Harries, A. Yde, C. Galinos, K. Hermans, J. B. de Vaal, P. Bozonnet, L. Buoy, I. Bayati, R. Bergua, J. Galvan, I. Mendikoa, C. B. Sanchez, H. Shin, S. Oh, C. Molins, and Y. Debruyne. OC5 Project Phase II: Validation of Global Loads of the DeepCwind Floating Semisubmersible Wind Turbine . *Energy Procedia*, vol. 137, pp. 38-57, 2017.

[20] A. N. Robertson, J. Jonkman, M. Masciola, H. Song, A. Goupee, A. Coulling, and C. Luan, "Definition of the semisubmersible floating system for phase II of OC4," *TP-5000-60601*, National Renewable Energy Laboratory, USA, September, 2014.

[21] D. M. Skene, N. Sergiienko, B. Ding, and B. Cazzolato, "The prospect of combining a point absorber wave energy converter with a floating offshore wind turbine," *Energies*, vol. 14, 7385, 2021.

[22] W. Shi, J. Li, C. Michailides, M. Chen, S. Wang, and X. Li., "Dynamic load effects and power performance of an integrated wind-wave energy system utilizing an optimum torus wave energy converter," *J. Mar. Sci. Eng.*, vol. 10, 1985, 2022.

[23] H. Kim, E. Min, S. Heo, and W. C. Koo, "Motion analysis of a wind-wave energy TLP platform considering second-order wave forces," *J. Ocean Eng. Tech.*, vol. 36(6), pp. 390-402, 2022.

[24] W. E. Cummins, "The impulse response function and ship motions," *Schiffstechnik*, vol. 47, pp. 101-109, 1962.

[25] T. S. Hallak, M. Kamarlouei, J. F. Gaspar, and C. Guedes Soares, "Time domain analysis of a conical point-absorber moving around a hinge," In *Trends in Maritime Technology and Engineering, Guedes Soares, C., Santos, T. A. (Eds.),* Taylor & Francis Group, vol. 2, pp. 401-409, 2022.